Atmospheric Pollution Research 15 (2024) 102105

Contents lists available at ScienceDirect

Atmospheric Pollution Research

journal homepage: www.elsevier.com/locate/apr

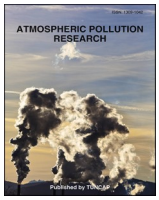

Air pollution biomonitoring in an urban-industrial setting (Taranto, Italy) using Mediterranean plant species

B. Cavazzin [a,*], C. MacDonell [a], N. Green [b], J.J. Rothwell [c]

[a] School of Geographical and Earth Sciences, University of Glasgow, Glasgow, G12 8QQ, Scotland, UK
[b] Department of Statistical Science, University College London, London, WC1E 6BT, UK
[c] Department of Geography, School of Environment, Education & Development, The University of Manchester, Manchester, M13 9PL, UK

ARTICLE INFO

Keywords:
Biomonitoring
Urban-industrial area
Indices of pollution
Spatial analysis

ABSTRACT

This study presents the first report on the elemental composition of five Mediterranean plant species (*Pinus pinaster*, *Eucalyptus camaldulensis*, *Nerium oleander*, *Olea europaea* and *Pittosporum heterophyllum*) to trace industrial emissions in Taranto, Italy, a mixed-use industrial and urban setting. Potential metal sources include vehicular traffic, steel and cement plants, and a petrochemical refinery. Samples were collected from 29 sites covering the Tamburi-Lido Azzurro neighbourhood and the historical quarter Città Vecchia-Borgo. High concentrations of toxic metals were observed in all samples, with marked inter-species variability. Model based clustering identified two distinct groups, one dominated by pine needles with higher metal concentrations than the other group composed of the other four plant species. The contamination factor (CF) and pollution load index (PLI) indices which use background samples to standardise the level of pollution, were used to remove species effect allowing for direct site comparison. Spatial analysis of CF and PLI data identified pollution hotspots near industrial areas and major roads, with areas of little to no air pollution near green spaces. Statistical analysis of the CFs revealed the contribution of different sources to element emissions. Ni and Cr were primarily emitted from the steel plant and petrochemical refinery, while Fe and Al were associated with road traffic emissions, and geogenic elements Ca, Mg, K, and Na were linked to marine spray and Saharan dust. This study demonstrates that combining multiple plant species with pollution indices can be a cost-effective biomonitoring approach for assessing air pollution and creating a high-density spatial monitoring network.

1. Introduction

Anthropogenic air pollution constitutes an increasing problematic and complex issue, with numerous studies having linked air pollution to detrimental effects on human health (Manisalidis et al., 2020; Mannucci and Franchini, 2017) and environmental impact such as acidification and toxification of sensitive ecosystems (Stevens et al., 2020). Air pollutants differ in their chemical composition, reaction properties, emission sources, ability to be transported, persistence in the environment and their impact on human health (Kampa and Castanas, 2008). Inorganic pollutants such as metals, are of interest because of their prolific presence in the urban environment (Gerdol et al., 2002; Zhang et al., 2018), and their properties as they are emitted in both elemental and compound forms. Metals have two main sources: natural (geogenic), and anthropogenic. A primary natural source is the erosion of the underlying and local rocks and the leaching of these metals into soils (Garrett, 2010). On a global scale, the main source of atmospheric mineral dust is the Sahara Desert which accounts for circa half of the annual mineral dust (Karanasiou et al., 2012). Sahara's dust directly affects the atmospheric particulate matter in the Mediterranean region (Flentje et al., 2015; Morales-Baquero et al., 2013; Theodosi et al., 2010). The main anthropogenic sources of metals in urban environments are dust dispersion from metal processing, fossil fuel combustion, vehicle exhaust, emission from cement factories, mining and other human activities (Alexandrino et al., 2020; Charron et al., 2019; Lehndorff and Schwark, 2010; Qu et al., 2013).

Indicators of changes resulting from environmental pollution in urban areas are an effective tool that can support decision making related to public health policy and environmental protection (Piazzetta et al., 2019). Biomonitors, top soils, street and road dust, atmospheric

Peer review under responsibility of Turkish National Committee for Air Pollution Research and Control.
* Corresponding author.
E-mail address: bianca.cavazzin@glasgow.ac.uk (B. Cavazzin).

https://doi.org/10.1016/j.apr.2024.102105
Received 25 October 2023; Received in revised form 1 March 2024; Accepted 1 March 2024
Available online 2 March 2024

deposition and particulate matter are amongst the most commonly used indicators (Abbasi et al., 2018; Fernández-Olmo et al., 2014; Modabberi et al., 2018). The first three are relatively inexpensive, applicable to large areas and timely alternatives for the analysis of the origin, distribution, and effects of urban pollution. With regards to the two latter, they require longer monitoring periods and are more resource intensive (Morera-Gómez et al., 2021). Biomonitoring is the use of vegetation as a passive sampler for air pollution. This approach has the advantage of high spatial resolution due to the availability of plants, low sampling costs, and it also provides the integrated effect of numerous environmental factors, including air pollution and weather conditions (Lehndorff and Schwark, 2010). Vascular plants are more representative of human experienced pollution (height 1.5/2m) in contrast with low vegetation types (height <1m) and conventional air pollution stations which are often fixed at heights >2.5m (Mitchell and Maher, 2009). Importantly, evergreen plants have been shown to capture more metal particles than broad-leaves species (Beckett et al., 2000). Of those evergreen plants, coniferous species have been proven to be more reliable than evergreen broadleaf trees due to higher deposition velocities for fine to ultrafine particulates and higher capture efficiency than their broadleaf counterparts (Lehndorff et al., 2006).

In the present study we focused on the industrial city of Taranto, Italy, which has mixed use industrial park located north of the city (Fig. 1). The district hosts an industrial and commercial port, food-processing factories, a steel plant, a cement plant and a petrochemical refinery. The city also harbours the main Italian navy base, military arsenal, and warship shipyard. Taranto's industrial activities (steel production in particular) have been under international scrutiny due to the large, unregulated emission of pollutants into the surrounding atmosphere. Similarly to other European countries, steel production in Taranto is carried out using an integrated steel process that includes coke ovens, sintering, blast furnaces, basic oxygen steelmaking, and finishing processes (Amodio et al., 2013).

According to the European Commission (2013), in the last 60 years Taranto's steel plant has consistently failed to meet the requirements set out by EU directives. Since the early 2000s the Regional Environmental Agency (ARPA) has been reporting that PM_{10}, $PM_{2.5}$, NO_2 and O_3 in the atmosphere do not meet the levels set by the 2008/50/EC EU directive. Industrial related emissions in Taranto include Fe, Mn, Zn, Pb and Ni, which have been associated with fossil fuels, petrochemical products, cement, and steel plants (Amodio et al., 2013; Di Gilio et al., 2017). Additionally, Cr is commonly used in Italy to produce ferrochromium and corrosion control in the steel industry (WHO, 2000). A study conducted by Viviano et al. (2005) on settled dust in the Tamburi-Lido Azzurro neighbourhood reported concentrations of polycyclic aromatic hydrocarbons (PAHs), As, Cd, Hg, and Ni higher than the levels set by the EU directives DM November 25, 1994 and 2004/107/CE.

The industrial and urban (traffic) components make this city a complex and critical setting to study. Despite the urgency, geochemical, environmental, and spatial studies in this area are scarce and no biomonitoring approaches have been used to date. In this study we deployed a biomonitoring approach, to characterize elemental composition of leaves of common Mediterranean tree species in the areas closest to the industrial park in Taranto; and subsequently trace their dispersion into the urban environments of the city.

2. Material and methods

2.1. Geography and geology of the study site

Taranto is a coastal city in the Apulia region, southern Italy (Fig. 1). It is the third largest city in Southern Italy, with an urban area expanding over 209 km^2 with a population of about 200,000. The climate of Taranto is semi-arid, typical of the Mediterranean region characterised by mild rainy winters and warm dry summers. The average annual rainfall amount is approx. 400 mm, with prevailing wind direction from NW (wind rose in Fig. 1). The dominant type of vegetation in the Apulia region is the Mediterranean macchia; characterised by evergreen shrubbery and garrigue such as *Arbutus unedo*, *Myrtus communis*, *Olea europaea*; pinewoods (e.g. *Pinus halepensis*, *Pinus Pinaster*) and palmettos (Campanile and Cocca, 2005; Costa and La Mantia, 2005). It is also common to find exotic plants, such as eucalyptus and oleander, typically used for urban landscaping in Mediterranean cities (Khattak and Jabeen, 2012).

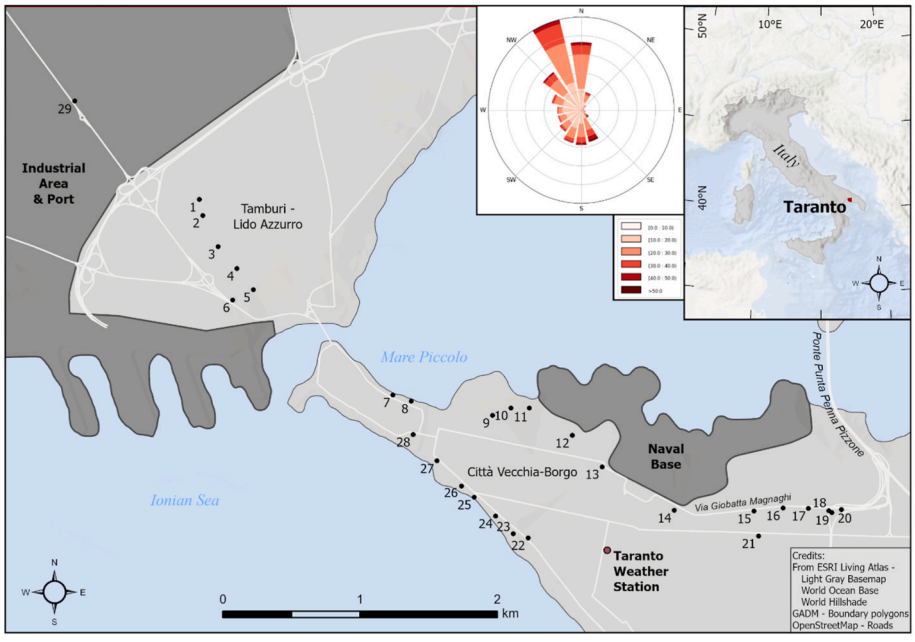

Fig. 1. Map showing the sampling sites of tree leaves and needles (1–29) within Taranto, along with the location of two major roads (Via Giobatta Magnaghi and Ponte Punta Penna Pizzone), industrial park, and naval base. Inset map: location of Taranto within Italy. The wind rose illustrates the daily average wind speed (in km/h) and direction for the period 2010–2023. Wind data collected from the Taranto weather station in the neighbourhood of Città Vecchia-Borgo (shown on the map) (wind data downloaded from visualcrossing.com).

A detailed description of the geology of the Gulf of Taranto and the Apulia region can be found in Bentivenga et al. (2004). Briefly, Taranto is located at the front of the southern Apennines belt which formed following the closure of the Mesozoic Tethys Ocean and subsequent deformation of the Adriatic passive margin during Tertiary and Quaternary. The front of the chain is partially overlaid by Pliocene – Pleistocene deposits, while the upper portion of the middle Pleistocene stratigraphy consists of marine sands and conglomerates arranged in several terraces (Massari and Parea, 1988).

2.2. Sampling

We collected 29 samples downwind (south-east) of the industrial park (Fig. 1) using a transect approach in a NW to SE direction. This covered the neighbourhood Tamburi-Lido Azzurro adjacent to the industrial park (sites 1 to 6 and 29) and the historical quarter Città Vecchia-Borgo (sites 7, to 28).

We also collected two background samples (B1a and B1b) in a wooded area *Bosco Sant'Antuono* North of Taranto (~20 km, see Supplementary Fig. S1 for location). In accordance with other studies, including those by Guéguen et al. (2011) and Kousehlar and Widom (2020) we selected background sites close to the study area, with a similar geologic setting. These sites are situated off-axis to the predominant wind direction in Taranto, thereby minimizing the impact of urban anthropogenic sources. However, we acknowledge that B1a and B1b may still be subject to some local/regional anthropogenic emissions.

Four evergreen species were selected for their high availability within the macchia vegetation and the urban test sites: maritime pine (*Pinus pinaster*), river red gum tree (*Eucalyptus camaldulensis*), oleander (*Nerium oleander*) and olive tree (*Olea europaea*). The tree species per site were selected according to their availability and are detailed in Table 1. Due to the lack of the selected tree species at site 14; the evergreen plant mock orange shrub (*Pittosporum heterophyllum*), was selected as a substitute. At each site GPS coordinates were recorded with a Garmin GPS 60 portable device.

Three to five leaf samples per tree were collected at adult head height (approx. 1.5–2m), to maximise any link between heavy metal concentrations and human impact. As surface deposits on evergreen leaves and needles typically showed a cumulative behaviour, i.e., an increase with the needle age (Krivan et al., 1987), during the sample collection older leaves and needles were preferentially samples to provide a more comprehensive picture of air pollution in Taranto. Sampling ensured that leaves and needles exposed to all wind direction were collected. Samples were placed in clean polyethylene bags, wrapped in aluminium foil, and refrigerated at 5 °C, before returning to the laboratory for analysis.

2.3. Laboratory analysis

Samples were freeze-dried for 18 h at −50 °C and subsequently weighted. The dry weight of each leaf/needle sample was used to normalize the final metal concentration per sample as indicated by Szönyi et al. (2008). The metal concentrations in this paper will be expressed in ppm (equivalent to μg/g of dry sediment) to allow for direct comparison with the literature. As washing could remove some elements from the leaves/needles surface (Boonpeng et al., 2017), unwashed samples were used for elemental analysis. The determination of metal concentration was conducted in accordance with the procedure outlined by Allan et al. (2013) and Krivan et al. (1987). Briefly, we submerged each sample in a microwave vessel with 20 ml of chloroform which was subsequently evaporated (open-top) in a SUB Aqua Pro (1 h at 88 °C). For sample digestion, leaves and needles where then removed from the container, the waxy layer of leaves was decomposed using an acid mixture of 69% v/v nitric acid (6.5 ml), 30% v/v hydrogen peroxide (3.5 ml). The vessels were sealed and placed in a CEM MARS Xpress microwave oven for 2 h. After digestion, the solutions were filtered with 540 Hardened Ashless Whatman filter papers and diluted to 25 ml with deionised water in volumetric glass flasks. A second dilution was achieved using 5 ml of the original solution further diluted to 20 ml with deionised water in new volumetric glass flasks. The final 20 ml solutions were transposed into 15 ml sterilised (new) conical centrifuge tubes and analysed with ICP-OES PerkinElmer Optima 2100DV to determine the metal concentrations following the parameters and calibration protocol described in Allan et al. (2013). Briefly, calibration curves for Al, Ca, Cd, Co, Cr, Cu, Fe, K, Mg, Mn, Na, Ni, Pb, Zn were constructed from standard solution of each element ranging from 0.001 mg/L to 1000 mg/L. We calculated the limits of detection (LOD) as three times the standard deviation of blank measurements (n 10) divided by the slope of the analytical curve. Similarly, the limits of quantification (LOQ) were calculated as ten times the standard deviation of 10 blank measurements divided by the slope of the analytical curve. The accuracy of the method was evaluated by the analysis of certified reference material Apple Leaves 1515a (National Institute of Standards and Technology, Gaithersburg, MD, USA). Digestion blank (i.e. digestion solution without plant material) was analysed following the same procedure used for the leaves/needles to check for any potential contamination. The metals concentration values at each site (see Supplementary Table S3) are reported as the mean of three samples analysed per site. Each sample was analysed in triplicate to ensure Relative Standard Deviation (RSD) values of <20%.

Table 1
List of tree species collected at each site, including background samples B1a and B1b.

Tree Species	Sites
Eucalyptus cam.	1, 2, 3, 6
Nerium oleander	7, 15, 16, 18, 21,22, 23, 24, 25, 26, 27, 29, B1b,
Olea europaea	5, 17
Pinus Pinaster	4, 8, 9, 10, 11, 12, 13, 19, 20, 28, B1a
Pittosporum het.	14

2.4. Statistical analysis

Model-based clustering was performed on the dataset of metal concentration for each tree-species to assess whether tree species showed different metal accumulation regimes and therefore grouped in different clusters. Model-based clustering assumes that the multivariate dataset consists of several clusters and that each cluster can be described by a Gaussian (i.e., normal) distribution; thus, the dataset can be expressed as a sample from a mixture of multivariate normal distributions (McLachlan et al., 2019). Model-based clustering incorporates a measure of uncertainty to the cluster assignments and provides soft assignment such that observations have a probability of belonging to each cluster rather than simply being assigned to the best fitting cluster (Fraley and Raftery, 2002). The model parameters are estimated using the Expectation-Maximization (EM) algorithm (Dempster et al., 1977). Each component k is centred at its means (μ_k), more certainty of cluster membership near the mean and other geometric features (shape, volume, orientation) of each cluster are determined by the covariance matrix (Σ_k) (Scrucca et al., 2016). For this analysis, we used R version 4.2.2 (R Core Team, 2022) and employed the package *Mclust* (v5.4.7; Scrucca et al., 2016), which uses maximum likelihood to fit multivariate models, with different covariance matrix parameterizations, for a range of k clusters. The best model is selected using the Bayesian Information Criterion (BIC) (Schwarz, 1978). BIC is a tool for model selection amongst a given set of models that considers goodness of fit, and the number of parameters used to achieve the fit (Schwarz, 1978). Additionally, we performed Principal Component Analysis (PCA) Pearson correlation test to assess the relationship between elements and to identify common pollution sources. PCA was performed using R

functions *prcomp*, and the R package *Hmisc* (Alzola and Harrell, 2006) was used to carry out a Pearson correlation analysis. Prior to statistical analysis, metal concentrations and CFs were logged and scaled to their means to reduce any bias caused by the different ranges of values. Logging the distribution reduces skewness, moving it closer normality, a requirement of the Pearson correlation coefficient (Ahlgren et al., 2003). Furthermore, adjusting by the mean and standard deviation ensures a comparable scale across all variables. As PCA may not be a suitable technique for data with skewed distribution or outliers (Maadooliat et al., 2015), transforming a variable's magnitude through scalar multiplication is a common method to produce distinct eigenvalues and eigenvectors (Huang et al., 2008).

2.5. Indices of pollution

To assess the degree of pollution, we used two indices which consider the concentration of an element in the context of background concentration: the contamination factor (CF) and pollution load index (PLI). The CF is useful to evaluate pollution by comparing the pre- and post-industrial levels of metals (Hakanson, 1980). CF is defined using Eq (1).

$$CF = \frac{\text{Measured concentration of element}}{\text{Background concentration of element}} \quad (1)$$

CF values are unitless and can be divided into four classes: no/low contamination ($CF < 1$), moderate contamination ($1 \leq CF < 3$), considerable contamination ($3 \leq CF < 6$), and very high contamination ($CF \geq 6$). PLI (Tomlinson et al., 1980), is useful to evaluate the general pollution effect of various elements at each site (Boonpeng et al., 2017). This index is defined by the following equation:

$$PLI = (CF_1 \text{ x } CF_2 \text{ x } \ldots \text{ } CF_n)^{(1/n)} \quad (2)$$

Where CF is the contamination factor for element *i=1, …n*. PLI values are unitless and fall into three categories: within the natural background level (PLI $\leq$0.7), warning line of pollution (0.7 < PLI $\leq$1), and deterioration quality (PLI >1) (Salazar-Rojas et al., 2023; Tomlinson et al., 1980).

2.6. Spatial analysis

Distribution patterns of elements as CF and PLI were mapped using Inverse Distance Weighting (IDW) interpolation method within ArcGIS Pro version 3.1, covering an area of 13.66 km^2. Interpolation uses points of known value to estimate the values for unsampled locations (Burrough et al., 2015). The IDW method gives greater weight to the value of points closest to the unsampled prediction location, and the weight reduces as a function of distance (Burrough et al., 2015; Longley et al., 2011). The following parameters were used for the interpolations: power of 2, all 29 sample points, and an output cell size of 1m. The IDW interpolation is mainly controlled by the power value (Burrough et al., 2015), which defines the smoothness of the interpolation. We used a power value of 2, which provides more localised values predictions, which has been shown to produce the most accurate estimates given the statistical properties of the sample values (Bargawa and Purnomo, 2016). Spatial analysis was used alongside PCA to identify pollution sources and to assess the areas with the highest vulnerability to air pollution.

3. Results and discussion

3.1. Elemental composition of tree leaves

Summary statistics for major and trace elements are listed in Table 2. The average concentration of major elements follows the sequence Ca > Na > Mg > K > Zn > Al > Fe (Table 2). The abundance of major elements in tree leaves is expected, as these elements are macronutrients of plants (White and Brown, 2010). A variety of other studies have also reported baseline high (>1000 ppm) concentrations of Ca, Mg and Na in different plant species including moss (Lazo et al., 2019), pine needles (Brown et al., 2017), lichens (Bergamaschi et al., 2007), fir and rhododendron (Sun et al., 2011).

The abundance of trace elements follows the sequence Cu > Cr > Ni > Mn > Pb > Co > Cd (Table 2). The average values determined for all trace elements in addition to Zn, Al and Fe fit levels characteristic of polluted urban regions affected by industrial and traffic related emissions including Cologne, Germany (Lehndorff and Schwark, 2010), Cienfuegos and Santa Clara, Cuba (Morera-Gómez et al., 2021), Cordoba, Argentina (Carreras and Pignata, 2002) and Middletown, Ohio (Kousehlar and Widom, 2020). The background samples contain the lowest abundances of Cd (B1) and Pb (B2) as they were below the limits of quantification, the other elements follow between the mean ± standard deviation of the sampling sites. Of the two background samples, B1 (pine needles) has higher concentration of all metals, except for Cd, relative to B1b (oleander).

3.2. Tree species effect

Fig. 2 shows the results of the model-based clustering performed on the tree-species per site plotted in a biplot. The best model of the cluster analysis base on BIC values (see Supplementary Fig. S2), identified two distinct clusters. Cluster 1 encompassing all the Eucalyptus, Oleander and Pittosporum samples and one sample of Olive tree. Cluster 2 includes all the *Pinus Pinaster* samples and one of Olive tree (site 17). The cluster analysis showed that there is a tree-species effect on leaf element concentration. This effect is likely due to the properties of pine needles, a phenomenon described in a variety of studies, where efficacious biomonitors due to their long and narrow structure increase the capture

Table 2
Summary statistics of the elemental composition (in ppm) of tree leaves samples from Taranto and background samples B1 and B1b. Also reported LOD and LOQ per element (ppm).

Element	Mean	Min	Max	St Dev	B1a	B1b	LOD	LOQ
Al	77.64	10.84	335.22	89.07	107.67	55.6	1.20	3.96
Ca	4892.42	651.93	20640.21	4897.34	11928.22	1697.95	2.56	8.45
Cd	0.17	0.07	0.51	0.15	–	0.42	0.02	0.06
Co	0.35	0.06	0.94	0.31	0.77	0.46	0.02	0.06
Cr	8.33	0.50	43.52	10.52	13.47	1.85	0.21	0.69
Cu	9.79	1.28	38.63	9.32	27.87	4.96	0.43	1.42
Fe	74.74	14.91	238.63	65.54	88.91	77.66	1.89	6.29
K	380.11	65.99	1583.74	345.93	734.77	108.88	1.15	3.79
Mg	1444.97	200.60	6120.14	1455.45	3578.26	438.3	1.04	3.43
Mn	2.67	0.65	8.13	2.06	4.01	1.49	0.18	0.59
Na	4655.70	620.70	19905.29	4735.54	11775.22	1393.58	0.97	3.20
Ni	3.85	0.21	41.53	8.29	3.75	0.83	0.05	0.16
Pb	0.56	0.19	1.07	0.33	1.81	–	0.05	0.16
Zn	83.17	9.74	300.28	73.44	218.25	34.28	1.07	3.53

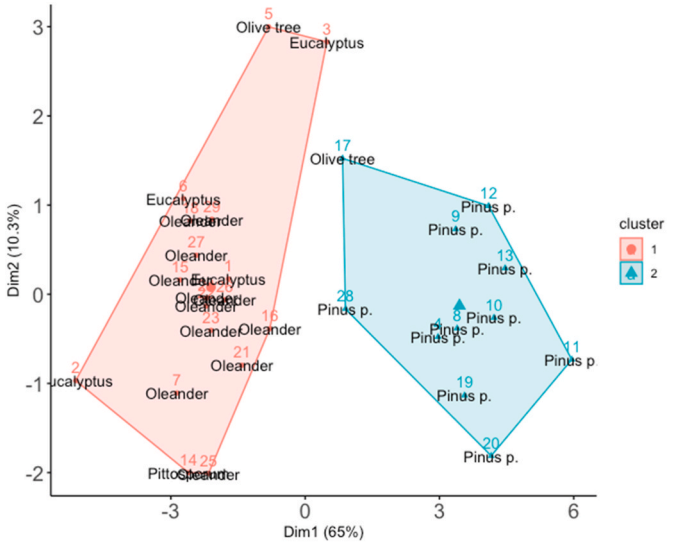

Fig. 2. Biplot of model-based clustering showing two distinct clusters. Cluster 1: Eucalyptus, Oleander and Pittosporum samples. Cluster 2: Pine and Olive tree samples.

efficiency and the deposition velocity of airborne particulates (Lehndorff et al., 2006; Lehndorff and Schwark, 2010).

The results of the present investigation agree with these previous studies, where *Pinus Pinaster* samples have the highest average concentration per element (see Supplementary Table S3). Site 17 falls within cluster 2, although its Euclidean distance to the centre of cluster 2 is only slightly shorter than cluster 1, suggesting that site 17 has characteristics of both clusters. This classification in cluster 2, represents the average high concentration of elements in site 17 likely due to its location, close to highly trafficked areas (*Ponte Punta Penna Pizzone* and *Via Giobatta Magnaghi*) which during sampling, were noted to be the points of maximum slow-moving or stationary traffic. In order to mitigate for the vegetation effect, CFs (for values see Supplementary Table S4) were used for subsequent spatial and statistical analysis instead of absolute element concentration. CFs were calculated using two different background samples: B1b (*Nerium oleander*) for cluster 1 and B1a (*Pinus Pinaster*) for cluster 2.

3.3. Sources of pollution

Fig. 3 shows the results of the PCA of CF, including the contribution

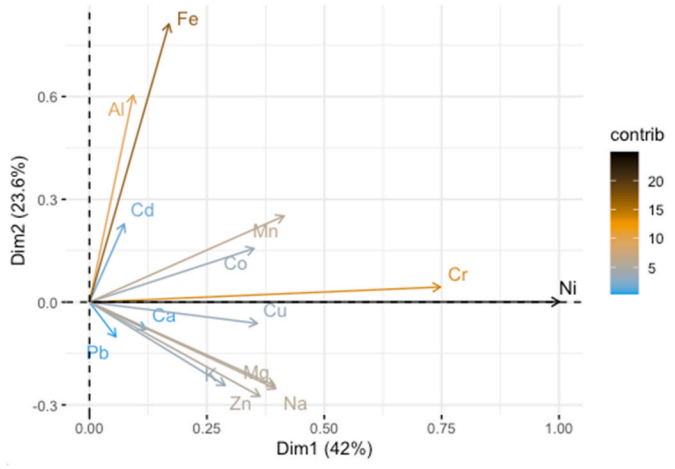

Fig. 3. PCA biplot of individual metals' CF. The legend shows the contribution of each CF to dimension 1 and 2.

of each element to dimensions (components) 1 and 2. PCA loadings also listed in Table 3. According to PCA statistical results, 65.6% of variance of elements' CF is explained by the first two components. The first component, explaining 42% of the variance, is dominated by Ni and Cr CF, which are also highly correlated to each other (Pearson's correlation = 0.83 $p < 0.01$, Table 4). The loading of Ni and Cr CF to the PCA, indicates a significant contribution of the industrial park (particularly the steel plant and the petrochemical refinery), to the pollution of Taranto. Ni is the most abundant metal in crude oil and has widely reported in the literature as indicative of the use of fossil fuels in power plants and metallurgical industries (Moreno et al., 2010; Morera-Gómez et al., 2021). Additionally, ferrochromium production used for stainless steel manufacturing and cement production are two main sources of European Cr emissions (Fahim et al., 2019; Tumolo et al., 2020).

Fe and Al CF contributed the most to the 2nd component which explained 23.6% of the total variance. Fe and Al emissions have been linked to metallurgy industry, however, in urban environments they are primarily related to resuspension of road dust (Chambers et al., 2016) and the wear of automotive parts (Fujiwara et al., 2011). Although disentangling the two sources is difficult, road traffic should be also considered as a potential source of metal emissions in Taranto. Of the geogenic elements, Na and Mg have the most loading on both dimensions. These two elements also have a strong and significant Pearson correlation coefficient of 1 ($p < 0.01$, Table 4), suggesting a common source of emission. According to Beckett et al. (2000) marine spray in coastal locations is accountable for the high concentrations of Na and Mg. Additionally, another significant natural source which affects the whole Mediterranean region and therefore Taranto, is Saharan dust. This dust is characterised by high Ca, Mg, K and Na concentrations (Flentje et al., 2015; Morales-Baquero et al., 2013). Marine aerosol and Saharan dust contribute up to 39% to atmospheric particles (PM_{10}) in the Mediterranean region (Scerri et al., 2016). These geogenic metals were observed to have relatively high concentrations in both urban and background samples, which suggests a widespread 'blanket' effect of marine spray and Saharan dust in both Taranto and the wider region.

3.4. Spatial assessment of pollution

To assess the spatial distribution of metal emissions, CFs for each element were plotted using IDW and are shown in Figs. 4 and 5. All 29 sites show contamination relative to the background levels, however, individual element's CF per site is location dependant. On average, Ni and Cr exhibited the highest CF values, followed by K, Mg, Na, Ca, and Mn. Ni and Cr show very high contamination near the industrial area (49.94 and 17.28, respectively). These values are much higher than the CF of Ni and Cr reported in other sites close to industrial complexes such as those of Boonpeng et al. (2017) (CF of Ni 2, CF of Cr 1.6). Our observations agree with the findings of Di Gilio et al. (2017) and Viviano et al. (2005) who reported high levels of Ni in settled dust and PM in the

Table 3
PCA loadings for components 1 and 2.

	Comp. 1	Comp. 2
CF Al	0.058	0.503
CF Ca	0.075	−0.066
CF Cd	0.046	0.190
CF Co	0.218	0.130
CF Cr	0.466	0.037
CF Cu	0.223	−0.052
CF Fe	0.106	0.676
CF K	0.180	−0.202
CF Mg	0.246	−0.203
CF Mn	0.258	0.209
CF Na	0.247	−0.210
CF Ni	0.624	0.001
CF Pb	0.035	−0.084
CF Zn	0.226	−0.229

Table 4
Pearson correlation between CF of elements measured in Taranto.

	Al	Ca	Cd	Co	Cr	Cu	Fe	K	Mg	Mn	Na	Ni	Pb	Zn
Al	1	0.07	0.38	0.11	0.1	0.25	0.78**	−0.13	−0.03	0.39*	−0.04	−0.05	−0.17	−0.03
Ca		1	0.26	0.27	0.31	0.62**	−0.19	0.56**	0.57**	0.17	0.57**	0.09	−0.02	0.58**
Cd			1	0.39*	0.12	0.16	0.32	0.02	0.02	0.29	0.02	−0.09	−0.13	0.15
Co				1	0.36	0.33	0.16	0.15	0.23	0.38*	0.24	0.26	−0.17	0.15
Cr					1	0.66**	0.25	0.47**	0.57**	0.71**	0.58*	0.83**	0.27	0.49**
Cu						1	0.06	0.68**	0.93**	0.55**	0.93**	0.43*	0.1	0.76**
Fe							1	−0.32	−0.24	0.62**	−0.26	0.17	−0.26	−0.32
K								1	0.8**	0.27	0.79**	0.33	0.32	0.72**
Mg									1	0.4*	1**	0.4*	0.24	0.83**
Mn										1	0.38*	0.63**	0.04	0.19
Na											1	0.39*	0.25	0.84**
Ni												1	0.13	0.37*
Pb													1	0.32
Zn														1

**$p < 0.01$.
*$p < 0.05$.

Tamburi-Lido Azzurro neighbourhood adjacent to the steel plant. This spatial pattern of high considerable to very high contamination in proximity of the industrial park is also observed for Cd, Co, Fe, Mn. As identified earlier, high pollution levels of Ni, Cr, Cd and Fe have been widely reported in the literature as indicative of the use of fossil fuels, presence of power plants and metallurgical industries (Carreras and Pignata, 2002). Here, the results show a clear influence of the industrial park emissions on the Taranto's area closest to the steel plant, cement plant and petrochemical refinery. Heavy metal particulates, especially Ni, of anthropogenic origin tend to be finer than those from natural sources and have a longer residence time in the atmosphere (Begum et al., 2022). This likely prolongs the exposure time of plants to pollutants, resulting in an increased accumulation of heavy metals in sites 1 to 6, close to the industrial park.

Spatial analysis shows that moderate to considerable contamination for Al, Fe, Mn, Zn and Cr, is also identified for sites 9 to 20, which are close to the Military arsenal and two major roads: *Via Giobatta Magnaghi* for sites 13 to 18, and the freeway *Ponte Punta Penna Pizzone* for sites 19 and 20 (see Fig. 1 for locations). The influence of the Military base on the on the urban air emissions is possible but unlikely as military shipbuilding activities have been moved to a new location south of Taranto in 2004. Traffic related emissions are more likely to be the cause of the contamination at these sites, as Mn, Fe, Al, Zn and Cr are linked to highly trafficked areas (Demková et al., 2019; Han et al., 2021), corroborating the results of the PCA and correlation analysis. The CF values for Zn, Cr, and Pb observed in proximity to busy roads agree with the CFs reported by Salazar-Rojas et al. (2023), ranging between <1 and < 4 for Cr, 0 and < 5 for Zn, and 0 and < 4 for Pb.

The traditionally geogenic element Ca show CF values similar to the background, moderate contamination is observed only for sites 1, 3, 5, close to the industrial park and 14 and 17, close to *Via Giobatta Magnaghi*. Ca enrichment in urban regions has been reported by an increasing number of studies which have shown high Ca concentrations even when the regions have no carbonate bedrock (Chambers et al., 2016; Kaushal et al., 2017; Washbourne et al., 2012). The accumulation of Ca in urban vegetation is mainly attributed to the widespread use of artificial Ca-rich materials, their weathering and resuspension, including concrete structures, construction and demolition wastes, and impervious surfaces (Chambers et al., 2016; Kaushal et al., 2017; Morera-Gómez et al., 2021). While Ca is not typically classified as a hazardous metal (Wu et al., 2018), its enrichment in urban areas has been shown to have adverse effects on the environment (Moore et al., 2013). These effects include the alteration of the cation exchange of shallow groundwater which affects plant communities (Moore et al., 2013), as well as the alteration of the pH of freshwater streams (Kaushal et al., 2017).

IDW was adopted to spatially assess PLI and identify the urban areas with the highest vulnerability to pollution (Fig. 6). PLI was calculated using the following metals: Al, Cd, Co, Cr, Cu, Fe, Mn, Ni, Pb, Zn. We omitted the elements Ca, Mg, K and Na due to their likely natural source, as previously discussed, which include marine spray (Beckett et al., 2000) and Saharan dust (Flentje et al., 2015; Morales-Baquero et al., 2013). The spatial analysis shows that the transects investigated in Taranto are, on average, within warning PLI values. Industrial and traffic emission effects are noticeable in three hotspots which are highly affected by heavy metal emissions and classified as in deterioration. The two hotspots (PLI >1) in the historical quarter, Città Vecchia-Borgo, are located close to two heavily trafficked streets (Via Giobatta Magnaghi and Ponte Punta Penna Pizzone), these areas are also characterised by closely packed tall residential buildings which hinder the natural circulation of air. This urban configuration is commonly referred to as 'street canyon' (Li et al., 2006) and is characterised by a distinct climate dominated by micro-scale meteorological processes (Oke, 1988), with air ventilation and pollutant removal occurring only at the roof level (Li et al., 2006). The street canyon effect can cause traffic emissions to become trapped at street-level, increasing the concentrations of pollution above background levels (Marini et al., 2015; Zhu et al., 2021). Our results indicate that in Taranto, a mixed urban-industrial environment, traffic is often the primarily source of pollution for sites adjacent to major roads. Our findings agree with those of Salo et al. (2012), who observed the highest PLI values (>1) in moss samples collected near major roads in an urban site affected by mixed pollution sources, including traffic and industrial activities (oil refineries, steel works and shipyards). A second degrading hotspot with PLI of 2.75 is observed in the Tamburi-Lido Azzurro neighbourhood, located less than 2 km from the industrial park. This area is characterised by very high pollution levels of Cr and Ni. Similar results have been presented by Boonpeng et al. (2017), who reported a PLI value of 2.1 in two sites located less than 4 km from a petrochemical industrial complex.

Sample 29, collected inside the industrial area, shows a PLI of 0.75, suggesting warning levels of pollution but not indicating deterioration. As site 29 is the only one collected from inside the industrial area, it may not be fully representative of the entire park. However, the relatively low PLI may be attributed to the building and space configuration of the industrial park, characterised by open spaces and low infrastructure. It is likely that the prevailing NW winds carry the pollution southwards toward the residential Tamburi-Lido Azzurro neighbourhood, where it accumulates. The interaction between urban configuration and wind patterns is a key factor affecting the dispersion trajectories of atmospheric particulate matter (Kumar et al., 2009; Mei et al., 2018). Layout differences, such as high-rise buildings near low-rise buildings, can significantly impact local air flow, accelerating the dispersion of pollutants (Hang et al., 2011). This effect is exacerbated by wind speed, which enhances particle transport and reduces local particle

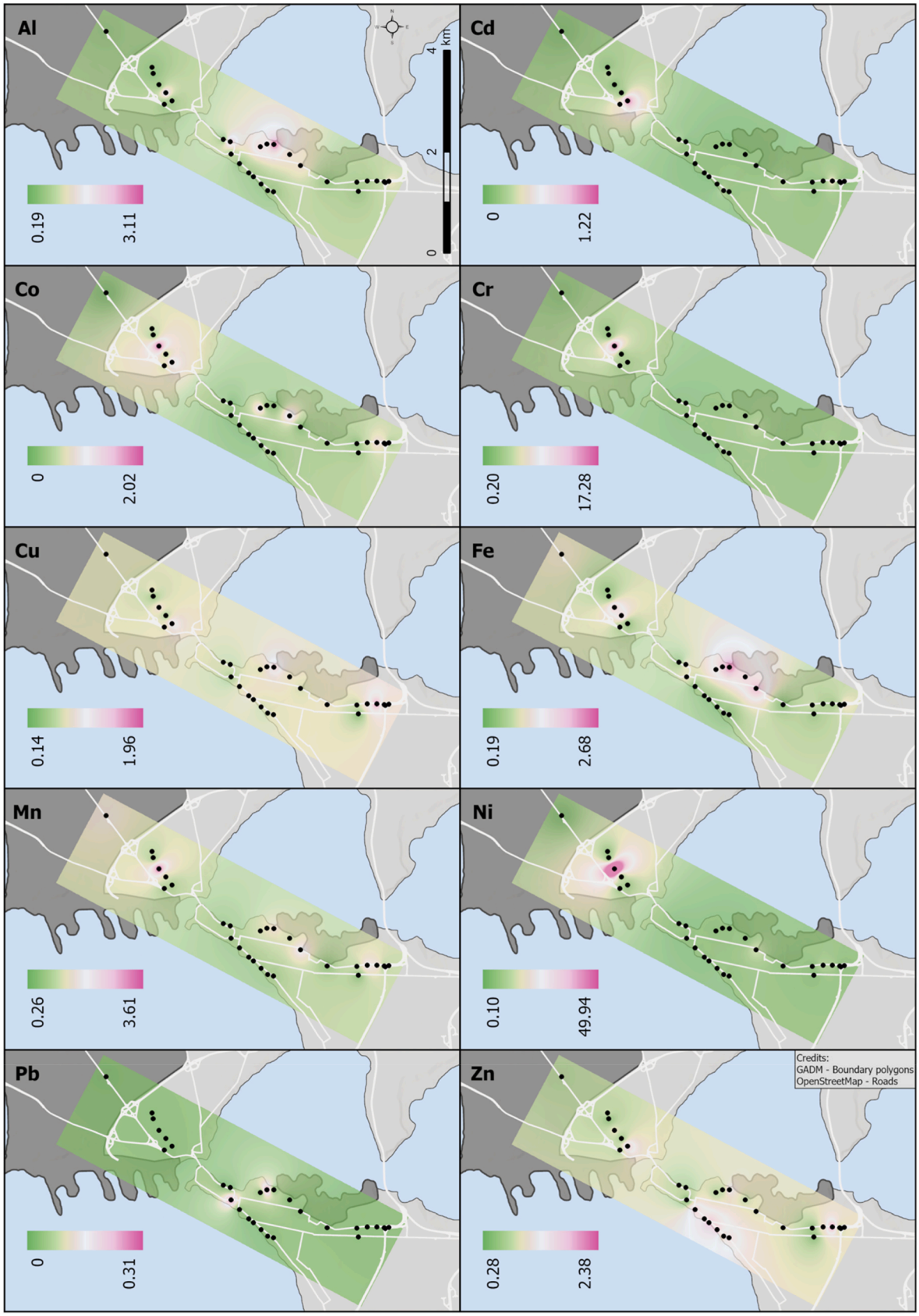

Fig. 4. Maps showing the spatial distribution of CF for (from top left) Al, Cd, Co, Cr, Cu, Fe, Mn, Ni, Pb, Zn within the study area based on the inverse distance weighing (IDW) analysis of the 29 sites in Taranto. Scale shown in the Al map.

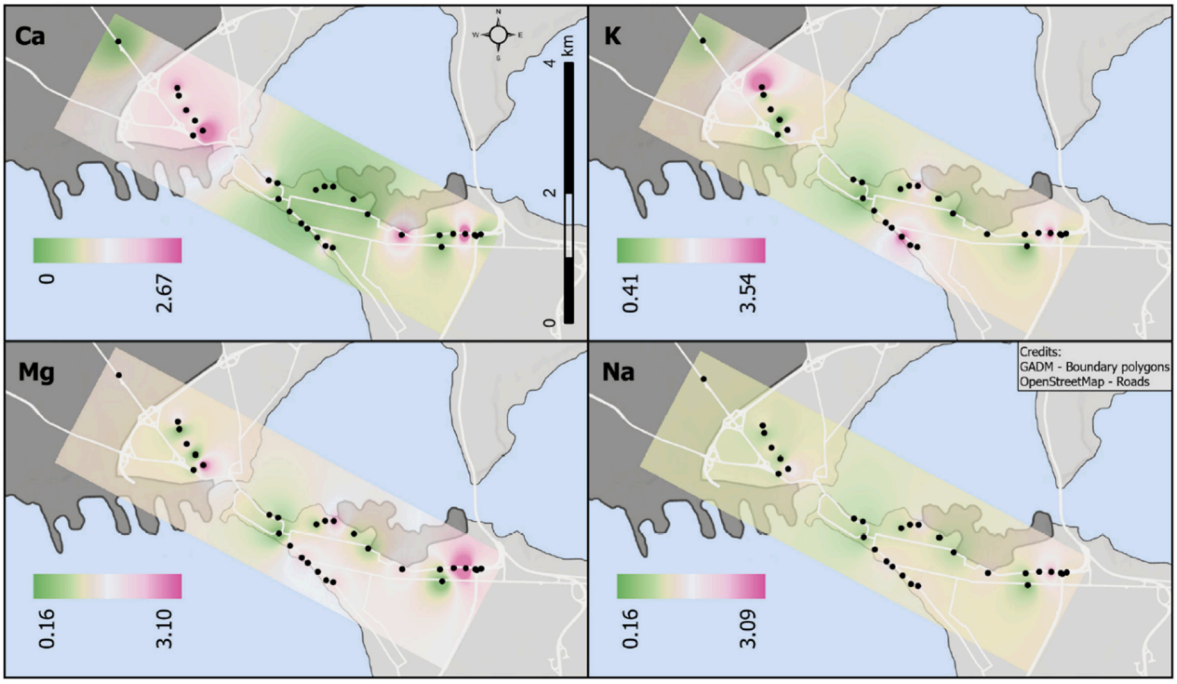

Fig. 5. Maps showing the spatial distribution of CF for Ca, K, Mg and Na within the study area based on the inverse distance weighing (IDW) analysis of the 29 sites in Taranto. Scale shown in the Ca map.

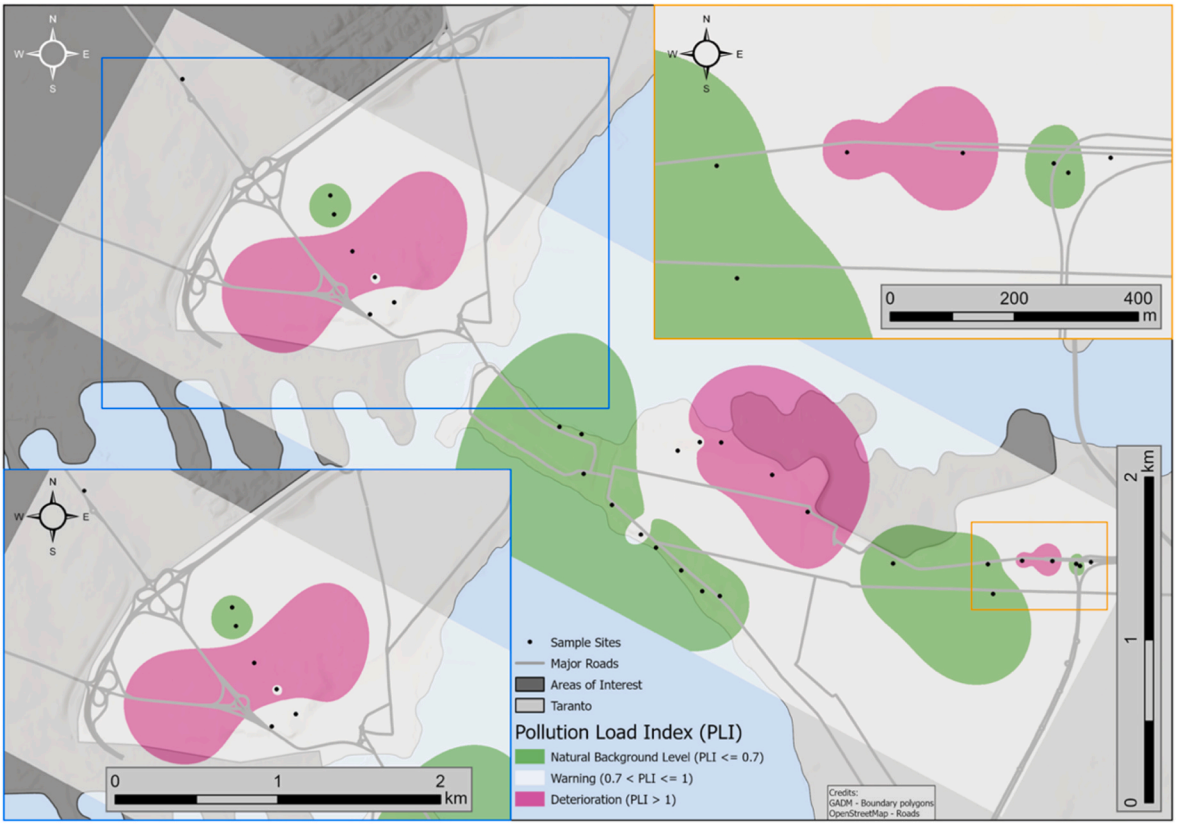

Fig. 6. Map showing the spatial distribution of PLI for the 29 sites within the study area based on the inverse distance weighing (IDW) analysis.

concentrations (Mei et al., 2018). The effect of wind on the level of pollution in the Tamburi-Lido Azzurro neighbourhood has also been observed by Di Gilio et al. (2017), who reported high concentrations of metals and PAHs in particulate matter in sites located downwind (south-east) of the steel plant, particularly for industrially emitted metals such as Fe, Mn, Zn, and Pb.

Low PLI values indicating no or low pollution in Taranto are found in or near urban green spaces, including parks and cemeteries. This effect is

evident in sites 1 and 2 (Fig. 4, blue inset), 17 and 19 (Fig. 4, yellow inset), as well as sites 22 to 28, 7 and 8, which are all close to community gardens and a cemetery. The importance of green spaces in urban settings has been documented in numerous studies, demonstrating that they may act as buffers and improve air quality compared to surrounding areas (Junior et al., 2022; Kruizse et al., 2019). Additionally, sites 22 to 28, 7 and 8 are likely influenced by their proximity to the sea, as a strong westerly sea breeze originates from the Ionian Sea (De Serio and Mossa, 2016). This breeze is likely to transport the pollutant east, away from these sites towards sites 9 to 13, where metal particulates accumulate.

4. Conclusion

This is the first known study deploying a multi-species biomonitoring approach to spatially assess the level of air pollution and identify the contribution of different sources to the air pollution in Taranto, Italy. We observed high concentrations of potentially toxic metals in all samples, but inter-species variability in elemental concentrations was evident. Model-based clustering identified two distinct groups, one dominated by pine needles with average higher metal concentrations than the other group composed of eucalyptus, oleander, olive tree and pittosporum. CF and PLI indices were employed to remove species effect in the subsequent statistical and spatial analysis. PCA and Pearson analysis suggested a significant contribution of the industrial park, particularly the steel plant and the petrochemical refinery, to the CF of Ni and Cr. CF values of Fe and Al were observed to be related to road traffic emissions, while geogenic elements Ca, Mg, K and Na CFs were associated with marine spray and Saharan dust. The spatial analysis performed on CFs was particularly useful in corroborating urban pollution sources, with the highest CF values observed for sites close to the industrial park (Ni, Cr, Cd, Co, Fe, Mn) and two major roads *Via Giobatta Magnaghi* and *Ponte Punta Penna Pizzone* for Al, Fe, Mn, Zn. PLI spatial analysis identified three hotspots of deteriorating conditions related to both traffic and industrial emission, as well as two areas of non-pollution. We suggest that urban settings, such as buildings and block configurations, exacerbate the concentration of air pollution, while green spaces and sites exposed to sea breeze are likely to experience reduced air pollution. The evidence presented here improves understanding of the spatial variability in pollution levels and sources in a mixed-use urban setting, achieved using a simple, cost-effective multi-species biomonitoring approach. The findings of this study provide further support for the growing use of evergreen plants as bioindicators, offering time-efficient, valuable tool for air quality monitoring in Mediterranean regions. Bioindicators, such as those deployed in this study, can help inform decision makers in the effective design of urban pollution mitigation strategies, such as increasing green space coverage and encouraging the effective air movement and circulation in dense urban settings.

CRediT authorship contribution statement

B. Cavazzin: Conceptualization, Methodology, Validation, Investigation, Formal analysis, Data curation, Writing – original draft. **C. MacDonell:** Visualization, Formal analysis, Writing – review & editing. **N. Green:** Formal analysis, Writing – review & editing. **J. Rothwell:** Methodology, Writing – review & editing.

Declaration of competing interest

The authors declare that they have no known competing financial interests or personal relationships that could have appeared to influence the work reported in this paper.

Acknowledgments

This research did not receive any specific grant from funding agencies in the public, commercial, or not-for-profit sectors. The authors would like to acknowledge laboratory technicians J. Yarwood and J. Moore, and G. Cavazzin and N.M. Durosini for fieldwork support. The authors also appreciate comments on the draft manuscript that were provided by L.A. Naylor and A. Hillier.

Appendix A. Supplementary data

Supplementary data to this article can be found online at https://doi.org/10.1016/j.apr.2024.102105.

References

Abbasi, S., Keshavarzi, B., Moore, F., Mahmoudi, M.R., 2018. Fractionation, source identification and risk assessment of potentially toxic elements in street dust of the most important center for petrochemical products, Asaluyeh County, Iran. Environ. Earth Sci. 77, 1–19. https://doi.org/10.1007/S12665-018-7854-Z/TABLES/5.

Ahlgren, P., Jarneving, B., Rousseau, R., 2003. Requirements for a cocitation similarity measure, with special reference to Pearson's correlation coefficient. J. Am. Soc. Inf. Sci. Technol. 54, 550–560. https://doi.org/10.1002/ASI.10242.

Alexandrino, K., Viteri, F., Rybarczyk, Y., Guevara Andino, J.E., Zalakeviciute, R., 2020. Biomonitoring of metal levels in urban areas with different vehicular traffic intensity by using Araucaria heterophylla needles. Ecol. Indicat. 117 https://doi.org/10.1016/J.ECOLIND.2020.106701.

Allan, A.N., Magalhães, T.A., Matos, W.O., Gouveia, S.T., Lopes, G.S., 2013. Characterization of carnauba wax inorganic content. J. Am. Oil Chem. Soc. 90, 1475–1483. https://doi.org/10.1007/S11746-013-2300-6.

Alzola, C., Harrell, F., 2006. An Introduction to S and the Hmisc and Design Libraries.

Amodio, M., Andriani, E., de Gennaro, G., di Gilio, A., Ielpo, P., Placentino, C.M., Tutino, M., 2013. How a steel plant affects air quality of a nearby urban area: a study on metals and PAH concentrations. Aerosol Air Qual. Res. 13, 497–508. https://doi.org/10.4209/AAQR.2012.09.0254.

Bargawa, W.S., Purnomo, H., 2016. Performance Evaluation of Ordinary Kriging and Inverse Distance Weighting Method for Nickel Laterite Resources Estimation.

Beckett, K.P., Freer-Smith, P., Taylor, G., 2000. Effective tree species for local air-quality management. Arboric. Urban For. 26, 12–19. https://doi.org/10.48044/JAUF.2000.002.

Begum, W., Rai, S., Banerjee, S., Bhattacharjee, S., Mondal, M.H., Bhattarai, A., Saha, B., 2022. A comprehensive review on the sources, essentiality and toxicological profile of nickel. RSC Adv. 12, 9139. https://doi.org/10.1039/D2RA00378C.

Bentivenga, M., Coltorti, M., Prosser, G., Tavarnelli, E., 2004. A new interpretation of terraces in the Taranto Gulf: the role of extensional faulting. Geomorphology 60, 383–402. https://doi.org/10.1016/J.GEOMORPH.2003.10.002.

Bergamaschi, L., Rizzio, E., Giaveri, G., Loppi, S., Gallorini, M., 2007. Comparison between the accumulation capacity of four lichen species transplanted to a urban site. Environ. Pollut. 148, 468–476. https://doi.org/10.1016/J.ENVPOL.2006.12.003.

Boonpeng, C., Polyiam, W., Sriviboon, C., Sangiamdee, D., Watthana, S., Nimis, P.L., Boonpragob, K., 2017. Airborne trace elements near a petrochemical industrial complex in Thailand assessed by the lichen Parmotrema tinctorum (Despr. ex Nyl.) Hale. Environ. Sci. Pollut. Control Ser. 24, 12393–12404. https://doi.org/10.1007/S11356-017-8893-9/TABLES/6.

Brown, G., Luu, I., O'Sullivan, G., Brown, G., Luu, I., O'Sullivan, G., 2017. Trace metal concentrations in pine needles at varying elevation in proximity to roadways in an urban environment. J. Environ. Protect. 8, 733–743. https://doi.org/10.4236/JEP.2017.86047.

Burrough, P.A., McDonnell, R.A., Lloyd, C.D., 2015. Principles of Geographical Information Systems, third ed. Oxford University Press.

Campanile, G., Cocca, C., 2005. Forests in the Apulia region: features and problems. Forest@ - Rivista di Selvicoltura ed Ecologia Forestale 2, 172–177. https://doi.org/10.3832/EFOR0274-002.

Carreras, H.A., Pignata, M.L., 2002. Biomonitoring of heavy metals and air quality in Cordoba City, Argentina, using transplanted lichens. Environ. Pollut. 117, 77–87. https://doi.org/10.1016/S0269-7491(01)00164-6.

Chambers, L.G., Chin, Y.P., Filippelli, G.M., Gardner, C.B., Herndon, E.M., Long, D.T., Lyons, W.B., Macpherson, G.L., McElmurry, S.P., McLean, C.E., Moore, J., Moyer, R. P., Neumann, K., Nezat, C.A., Soderberg, K., Teutsch, N., Widom, E., 2016. Developing the scientific framework for urban geochemistry. Appl. Geochem. 67, 1–20. https://doi.org/10.1016/J.APGEOCHEM.2016.01.005.

Charron, A., Polo-Rehn, L., Besombes, J.L., Golly, B., Buisson, C., Chanut, H., Marchand, N., Guillaud, G., Jaffrezo, J.L., 2019. Identification and quantification of particulate tracers of exhaust and non-exhaust vehicle emissions. Atmos. Chem. Phys. 19, 5187–5207. https://doi.org/10.5194/ACP-19-5187-2019.

Costa, C., La Mantia, L.M., 2005. Il ruolo della macchia mediterranea nel sequestro del carbonio. Forest@ - Journal of Silviculture and Forest Ecology 2, 378. https://doi.org/10.3832/EFOR0319-0020378.

De Serio, F., Mossa, M., 2016. Environmental monitoring in the mar grande basin (Ionian Sea, southern Italy). Environ. Sci. Pollut. Control Ser. 23, 12662–12674. https://doi.org/10.1007/S11356-015-4814-Y/FIGURES/11.

Demková, L., Oboňa, J., Árvay, J., Michalková, J., Lošák, T., 2019. Biomonitoring road dust pollution along streets with various traffic densities. Pol. J. Environ. Stud. 28, 3687–3696. https://doi.org/10.15244/PJOES/97354.

Dempster, A.P., Laird, N.M., Rubin, D.B., 1977. Maximum likelihood from incomplete data via the EM algorithm. J. Roy. Stat. Soc. B 39, 1–22. https://doi.org/10.1111/J.2517-6161.1977.TB01600.X.

Di Gilio, A., Farella, G., Marzocca, A., Giua, R., Assennato, G., Tutino, M., De Gennaro, G., 2017. Indoor/outdoor air quality assessment at school near the steel plant in Taranto (Italy). Advances in Meteorology 2017. https://doi.org/10.1155/2017/1526209.

Fahim, A., Dean, A.E., Thomas, M.D.A., Moffatt, E.G., 2019. Corrosion resistance of chromium-steel and stainless steel reinforcement in concrete. Mater. Corros. 70, 328–344. https://doi.org/10.1002/MACO.201709942.

Fernández-Olmo, I., Puente, M., Montecalvo, L., Irabien, A., 2014. Source contribution to the bulk atmospheric deposition of minor and trace elements in a Northern Spanish coastal urban area. Atmos. Res. 80–91. https://doi.org/10.1016/J.ATMOSRES.2014.04.002, 145–146.

Flentje, H., Briel, B., Beck, C., Collaud Coen, M., Fricke, M., Cyrys, J., Gu, J., Pitz, M., Thomas, W., 2015. Identification and monitoring of Saharan dust: an inventory representative for south Germany since 1997. Atmos. Environ. 109, 87–96. https://doi.org/10.1016/J.ATMOSENV.2015.02.023.

Fraley, C., Raftery, A.E., 2002. Model-based clustering, discriminant analysis, and density estimation. J. Am. Stat. Assoc. 97, 611–631. https://doi.org/10.1198/016214502760047131.

Fujiwara, F., Rebagliati, R.J., Dawidowski, L., Gómez, D., Polla, G., Pereyra, V., Smichowski, P., 2011. Spatial and chemical patterns of size fractionated road dust collected in a megacitiy. Atmos. Environ. 45, 1497–1505. https://doi.org/10.1016/J.ATMOSENV.2010.12.053.

Garrett, R.G., 2010. Natural Sources of Metals to the Environment, pp. 945–963. https://doi.org/10.1080/10807030911243836.

Gerdol, R., Bragazza, L., Marchesini, R., Medici, A., Pedrini, P., Benedetti, S., Bovolenta, A., Coppi, S., 2002. Use of moss (Tortula muralis Hedw.) for monitoring organic and inorganic air pollution in urban and rural sites in Northern Italy. Atmos. Environ. 36, 4069–4075. https://doi.org/10.1016/S1352-2310(02)00298-4.

Guéguen, F., Stille, P., Millet, M., 2011. Air quality assessment by tree bark biomonitoring in urban, industrial and rural environments of the Rhine Valley: PCDD/Fs, PCBs and trace metal evidence. Chemosphere 85, 195–202. https://doi.org/10.1016/J.CHEMOSPHERE.2011.06.032.

Hakanson, L., 1980. An ecological risk index for aquatic pollution control.a sedimentological approach. Water Res. 14, 975–1001. https://doi.org/10.1016/0043-1354(80)90143-8.

Han, K., Ran, Z., Wang, X., Wu, Q., Zhan, N., Yi, Z., Jin, T., 2021. Traffic-related organic and inorganic air pollution and risk of development of childhood asthma: a meta-analysis. Environ. Res. 194 https://doi.org/10.1016/J.ENVRES.2020.110493.

Hang, J., Li, Y., Sandberg, M., 2011. Experimental and numerical studies of flows through and within high-rise building arrays and their link to ventilation strategy. J. Wind Eng. Ind. Aerod. 99, 1036–1055. https://doi.org/10.1016/J.JWEIA.2011.07.004.

Huang, J.Z., Shen, H., Buja, A., 2008. Functional Principal Components Analysis via Penalized Rank One Approximation, pp. 678–695. https://doi.org/10.1214/08-EJS2182.

Junior, D.P.M., Bueno, C., da Silva, C.M., 2022. The effect of urban green spaces on reduction of particulate matter concentration. Bull. Environ. Contam. Toxicol. 108, 1104–1110. https://doi.org/10.1007/S00128-022-03460-3/TABLES/2.

Kampa, M., Castanas, E., 2008. Human health effects of air pollution. Environ. Pollut. 151, 362–367. https://doi.org/10.1016/J.ENVPOL.2007.06.012.

Karanasiou, A., Moreno, N., Moreno, T., Viana, M., de Leeuw, F., Querol, X., 2012. Health effects from Sahara dust episodes in Europe: literature review and research gaps. Environ. Int. 47, 107–114. https://doi.org/10.1016/J.ENVINT.2012.06.012.

Kaushal, S.S., Duan, S., Doody, T.R., Haq, S., Smith, R.M., Newcomer Johnson, T.A., Newcomb, K.D., Gorman, J., Bowman, N., Mayer, P.M., Wood, K.L., Belt, K.T., Stack, W.P., 2017. Human-accelerated weathering increases salinization, major ions, and alkalinization in fresh water across land use. Appl. Geochem. 83, 121–135. https://doi.org/10.1016/J.APGEOCHEM.2017.02.006.

Khattak, M.I., Jabeen, R., 2012. Detection of heavy metals in leaves of Melia azedarach and Eucalyptus citriodora as biomonitoring tools in the region of Quetta valley. Pakistan J. Bot. 44, 675–681.

Kousehlar, M., Widom, E., 2020. Identifying the sources of air pollution in an urban-industrial setting by lichen biomonitoring - a multi-tracer approach. Appl. Geochem. 121, 104695 https://doi.org/10.1016/J.APGEOCHEM.2020.104695.

Krivan, V., Schaldach, G., Hausbeck, R., 1987. Interpretation of element analyses of spruce-needle tissue falsified by atmospheric surface deposition. Naturwissenschaften 1987 74, 242–245. https://doi.org/10.1007/BF00424595, 5 74.

Kruizse, H., van der Vliet, N., Staatsen, B., Bell, R., Chiabai, A., Muiños, G., Higgins, S., Quiroga, S., Martinez-Juarez, P., Yngwe, M.A., Tsichlas, F., Karnaki, P., Lima, M.L., de Jalón, S.G., Khan, M., Morris, G., Stegeman, I., 2019. Urban green space: creating a triple win for environmental sustainability, health, and health equity through behavior change. Int. J. Environ. Res. Publ. Health 16, 4403. https://doi.org/10.3390/IJERPH16224403.

Kumar, P., Fennell, P.S., Hayhurst, A.N., Britter, R.E., 2009. Street versus rooftop level concentrations of fine particles in a Cambridge street canyon. Boundary-Layer Meteorol. 131, 3–18. https://doi.org/10.1007/S10546-008-9300-3/METRICS.

Lazo, P., Stafilov, T., Qarri, F., Allajbeu, S., Bekteshi, L., Frontasyeva, M., Harmens, H., 2019. Spatial distribution and temporal trend of airborne trace metal deposition in Albania studied by moss biomonitoring. Ecol. Indicat. 101, 1007–1017. https://doi.org/10.1016/J.ECOLIND.2018.11.053.

Lehndorff, E., Schwark, L., 2010. Biomonitoring of air quality in the Cologne Conurbation using pine needles as a passive sampler – Part III: major and trace elements. Atmos. Environ. 44, 2822–2829. https://doi.org/10.1016/J.ATMOSENV.2010.04.052.

Lehndorff, E., Urbat, M., Schwark, L., 2006. Accumulation histories of magnetic particles on pine needles as function of air quality. Atmos. Environ. 40, 7082–7096. https://doi.org/10.1016/J.ATMOSENV.2006.06.008.

Li, X.X., Liu, C.H., Leung, D.Y.C., Lam, K.M., 2006. Recent progress in CFD modelling of wind field and pollutant transport in street canyons. Atmos. Environ. 40, 5640–5658. https://doi.org/10.1016/J.ATMOSENV.2006.04.055.

Longley, P.A., Goodchild, M.F., Maguire, D.J., Rhind, D.W., 2011. Geographic Information Systems and Science, third ed. John Wiley & Sons, Hoboken.

Maadooliat, M., Huang, J.Z., Hu, J., 2015. Integrating data transformation in principal components analysis. J. Comput. Graph Stat. 24, 84. https://doi.org/10.1080/10618600.2014.891461.

Manisalidis, I., Stavropoulou, E., Stavropoulos, A., Bezirtzoglou, E., 2020. Environmental and health impacts of air pollution: a review. Front. Public Health 8, 505570. https://doi.org/10.3389/FPUBH.2020.00014/BIBTEX.

Mannucci, P.M., Franchini, M., 2017. Health effects of ambient air pollution in developing countries. International Journal of Environmental Research and Public Health 2017 14 (1048 14), 1048. https://doi.org/10.3390/IJERPH14091048.

Marini, S., Buonanno, G., Stabile, L., Avino, P., 2015. A benchmark for numerical scheme validation of airborne particle exposure in street canyons. Environ. Sci. Pollut. Control Ser. 22, 2051–2063. https://doi.org/10.1007/S11356-014-3491-6/FIGURES/11.

Massari, F., Parea, G.C., 1988. Progradational gravel beach sequences in a moderate- to high-energy, microtidal marine environment. Sedimentology 35, 881–913. https://doi.org/10.1111/J.1365-3091.1988.TB01737.X.

McLachlan, G.J., Lee, S.X., Rathnayake, S.I., 2019. Finite Mixture Models, pp. 355–378. https://doi.org/10.1146/annurev-statistics-031017-1003256.

Mei, D., Wen, M., Xu, X., Zhu, Y., Xing, F., 2018. The influence of wind speed on airflow and fine particle transport within different building layouts of an industrial city. J. Air Waste Manag. Assoc. 68, 1038–1050. https://doi.org/10.1080/10962247.2018.1465487.

Mitchell, R., Maher, B.A., 2009. Evaluation and application of biomagnetic monitoring of traffic-derived particulate pollution. Atmos. Environ. 43, 2095–2103. https://doi.org/10.1016/J.ATMOSENV.2009.01.042.

Modabberi, S., Tashakor, M., Sharifi Soltani, N., Hursthouse, A.S., 2018. Potentially toxic elements in urban soils: source apportionment and contamination assessment. Environ. Monit. Assess. 190, 1–18. https://doi.org/10.1007/S10661-018-7066-8/FIGURES/6.

Moore, J., Lev, S.M., Casey, R.E., 2013. Modeling the effects of road salt on soil, aquifer, and stream chemistry. In: Conference Proceedings for MODFLOW and More. Colorado School of Mines, Golden, CO 5.

Morales-Baquero, R., Pulido-Villena, E., Reche, I., 2013. Chemical signature of Saharan dust on dry and wet atmospheric deposition in the south-western Mediterranean region. Tellus B 65. https://doi.org/10.3402/TELLUSB.V65I0.18720.

Moreno, T., Querol, X., Alastuey, A., de la Rosa, J., Sánchez de la Campa, A.M., Minguillón, M.C., Pandolfi, M., González-Castanedo, Y., Monfort, E., Gibbons, W., 2010. Variations in vanadium, nickel and lanthanoid element concentrations in urban air. Sci. Total Environ. 408, 4569–4579. https://doi.org/10.1016/J.SCITOTENV.2010.06.016.

Morera-Gómez, Y., Alonso-Hernández, C.M., Armas-Camejo, A., Viera-Ribot, O., Morales, M.C., Alejo, D., Elustondo, D., Lasheras, E., Santamaría, J.M., 2021. Pollution monitoring in two urban areas of Cuba by using Tillandsia recurvata (L.) L. and top soil samples: spatial distribution and sources. Ecol. Indicat. 126, 107667 https://doi.org/10.1016/J.ECOLIND.2021.107667.

Oke, T.R., 1988. Street design and urban canopy layer climate. Energy Build. 11, 103–113. https://doi.org/10.1016/0378-7788(88)90026-6.

Piazzetta, K.D., Ramsdorf, W.A., Maranho, L.T., 2019. Use of airplant Tillandsia recurvata L., Bromeliaceae, as biomonitor of urban air pollution. Aerobiologia 35, 125–137. https://doi.org/10.1007/S10453-018-9545-3/FIGURES/4.

Qu, M.K., Li, W.D., Zhang, C.R., Wang, S.Q., Yang, Y., He, L.Y., 2013. Source apportionment of heavy metals in soils using multivariate statistics and geostatistics. Pedosphere 23, 437–444. https://doi.org/10.1016/S1002-0160(13)60036-3.

R Core Team, 2022. R: A Language and Environment for Statistical Computing. R Foundation for Statistical Computing, Vienna, Austria. URL. https://www.R-project.org/.

Salazar-Rojas, T., Cejudo-Ruiz, F.R., Gutiérrez-Soto, M.V., Calvo-Brenes, G., 2023. Assessing heavy metal pollution load index (PLI) in biomonitors and road dust from vehicular emission by magnetic properties modeling. Environ. Sci. Pollut. Control Ser. 30, 91248–91261. https://doi.org/10.1007/S11356-023-28758-5/TABLES/9.

Salo, H., Bućko, M.S., Vaahtovuo, E., Limo, J., Mäkinen, J., Pesonen, L.J., 2012. Biomonitoring of air pollution in SW Finland by magnetic and chemical measurements of moss bags and lichens. J. Geochem. Explor. 115, 69–81. https://doi.org/10.1016/J.GEXPLO.2012.02.009.

Scerri, M.M., Kandler, K., Weinbruch, S., 2016. Disentangling the contribution of Saharan dust and marine aerosol to PM10 levels in the Central Mediterranean. Atmos. Environ. 147, 395–408. https://doi.org/10.1016/J.ATMOSENV.2016.10.028.

Schwarz, G., 1978. Estimating the Dimension of a Model, pp. 461–464. https://doi.org/10.1214/aos/11763441366.

Scrucca, L., Fop, M., Murphy, T.B., Raftery, A.E., 2016. Mclust 5: clustering, classification and density estimation using Gaussian finite mixture models. R Journal 8, 289–317. https://doi.org/10.32614/RJ-2016-021.

Stevens, C.J., Bell, J.N.B., Brimblecombe, P., Clark, C.M., Dise, N.B., Fowler, D., Lovett, G.M., Wolseley, P.A., 2020. The impact of air pollution on terrestrial

managed and natural vegetation. Philosophical Transactions of the Royal Society A 378. https://doi.org/10.1098/RSTA.2019.0317.

Sun, S.Q., Wu, Y.H., Zhou, J., Yu, D., Luo, J., Bing, H.J., 2011. Comparison of element concentrations in fir and rhododendron leaves and twigs along an altitudinal gradient. Environ. Toxicol. Chem. 30, 2608–2619. https://doi.org/10.1002/ETC.661.

Szönyi, M., Sagnotti, L., Hirt, A.M., 2008. A refined biomonitoring study of airborne particulate matter pollution in Rome, with magnetic measurements on Quercus Ilex tree leaves. Geophys. J. Int. 173, 127–141. https://doi.org/10.1111/J.1365-246X.2008.03715.X.

Theodosi, C., Markaki, Z., Tselepides, A., Mihalopoulos, N., 2010. The significance of atmospheric inputs of soluble and particulate major and trace metals to the eastern Mediterranean seawater. Mar. Chem. 120, 154–163. https://doi.org/10.1016/J.MARCHEM.2010.02.003.

Tomlinson, D.L., Wilson, J.G., Harris, C.R., Jeffrey, D.W., 1980. Problems in the assessment of heavy-metal levels in estuaries and the formation of a pollution index. Helgol. Meeresunters. 33, 566–575. https://doi.org/10.1007/BF02414780/METRICS.

Tumolo, M., Ancona, V., De Paola, D., Losacco, D., Campanale, C., Massarelli, C., Uricchio, V.F., 2020. Chromium pollution in European water, sources, health risk, and remediation strategies: an overview. Int. J. Environ. Res. Publ. Health 17, 1–25. https://doi.org/10.3390/IJERPH17155438.

Viviano, G., Ziemacki, G., Settimo, G., Cattani, G., Spartera, M., Catucci, F., Carbotti, G., 2005. Air quality assessment in an urban-industrial area: the Taranto case study. Epidemiol. Prev. 45–49.

Washbourne, C.L., Renforth, P., Manning, D.A.C., 2012. Investigating carbonate formation in urban soils as a method for capture and storage of atmospheric carbon. Sci. Total Environ. 431, 166–175. https://doi.org/10.1016/J.SCITOTENV.2012.05.037.

White, P.J., Brown, P.H., 2010. Plant nutrition for sustainable development and global health. Ann. Bot. 105, 1073. https://doi.org/10.1093/AOB/MCQ085.

Wu, P., Yin, A., Fan, M., Wu, J., Yang, X., Zhang, H., Gao, C., 2018. Phosphorus dynamics influenced by anthropogenic calcium in an urban stream flowing along an increasing urbanization gradient. Landsc. Urban Plann. 177, 1–9. https://doi.org/10.1016/J.LANDURBPLAN.2018.04.005.

Zhang, R., Sun, X., Shi, A., Huang, Y., Yan, J., Nie, T., Yan, X., Li, X., 2018. Secondary inorganic aerosols formation during haze episodes at an urban site in Beijing, China. Atmos. Environ. 177, 275–282. https://doi.org/10.1016/J.ATMOSENV.2017.12.031.

Zhu, L., Ranasinghe, D., Chamecki, M., Brown, M.J., Paulson, S.E., 2021. Clean air in cities: impact of the layout of buildings in urban areas on pedestrian exposure to ultrafine particles from traffic. Atmos. Environ. 252, 118267 https://doi.org/10.1016/J.ATMOSENV.2021.118267.